Original Article

Effects of Fractionated Radiation on Murine Glioma Stem Cell Metabolism

Satoshi Fujita[1,2] Satoru Osuka[1] Shunsuke Shibao[1]
Kaori Igarashi[3] Tomoyoshi Soga[3] and Oltea Sampetrean[1]*

[1]Division of Gene Regulation, Institute for Advanced Medical Research, School of Medicine, Keio University
[2]Department of Neurosurgery (Ohashi), School of Medicine, Faculty of Medicine, Toho University
[3]Institute for Advanced Biosciences, Keio University

ABSTRACT

Background: Glioma stem cells (GSCs) have an important role in tumor recurrence after treatment. We recently showed that, in a mouse model of glioma, GSCs adapt to repeated radiation exposures by changing their secretory profile and modulating survival signaling. Irradiated GSCs also reduce their rate of proliferation. In the present study we examined whether these changes require a specific adaptation of GSC energy metabolism.

Methods: Initial tumors were established in mice by orthotopic implantation of *Ink4a/Arf*-null neural stem cells transduced with human $HRAS^{V12}$. GSCs isolated from the tumors were exposed (or not) to fractionated radiation (12 fractions of 5 Gy), and five clones in each group of cells were assessed for glucose consumption, lactate production, and content of intracellular metabolites.

Results: Rates of glucose consumption and lactate production were lower in clones exposed to radiation than in nonirradiated clones, which suggests a reduction in glycolysis. Among intracellular metabolites, the high concentrations of intermediates of glycolysis and nucleoside metabolism were reduced in irradiated clones, whereas levels of essential amino acids were largely unchanged.

Conclusions: Repeated radiation changes the metabolic preferences of GSCs, in conjunction with their slowed proliferation. Future studies should thus investigate intra- and extracellular metabolites, to identify potential diagnostic and therapeutic targets for glioma recurrence.

Toho J Med 2 (2): 45–52, 2016

KEYWORDS: glioma stem cell, radiation, metabolism, glycolysis, adaptation

Tumor recurrence after initial treatment is a major therapeutic challenge in malignant glioma. Recurrent lesions are initiated by a small number of tumor stem cells, which have greater self-renewal and tumorigenic capacities and tend to be more refractory to additional interventions as compared with most cells of the initial tumor. These glioma stem cells (GSCs) also pose a diagnostic challenge, as they must be detected within a treatment-altered environment and distinguished from pseudoprogression. Whereas radiological assessment by contrast-enhanced

1) 35 Shinanomachi, Shinjuku, Tokyo 160–8582, Japan
2) 2–17–6 Ohashi, Meguro, Tokyo 153–8515, Japan
3) 14–1 Baba, Tsuruoka, Yamagata 997–0035, Japan
*Corresponding Author: tel: +81–(0)3–5363–3983
e-mail: oltea@a6.keio.jp

DOI: 10.14994/tohojmed.2016.006
Received Feb. 22, 2016: Accepted Mar. 15, 2016
Toho Journal of Medicine 2 (2), June 1, 2016.
ISSN 2189–1990, CODEN: TJMOA2

magnetic resonance imaging remains the preferred follow-up method for malignant glioma, application of positron emission tomography (PET) or magnetic resonance spectroscopy to detect metabolically active tumor cells is also a common approach for identifying recurrences.[1]

Most tumor cells of solid malignancies are highly proliferative and derive their energy from aerobic glycolysis, a phenomenon known as the Warburg effect.[2,3] The metabolism of the stem cell pool, however, remains poorly understood for most types of cancer. GSCs have been reported to include subtypes with high glycolytic activity[4] and to utilize oxidative phosphorylation to a greater extent than their differentiated counterparts.[5] Using a mouse model, we previously showed that individual glioma stem-like cells in nontreated tumors can utilize either pathway.[6] However, we also found that, after exposure to fractionated radiation, stem cells adapt and become less proliferative and more radioresistant, and that these characteristics result in part from up-regulation of insulin-like growth factor 1 receptor (IGF1R) expression and down-regulation of kinase AKT activity.[7] The slowed proliferation of radioresistant stem cells suggests that these changes also require a specific adaptation of energy metabolism. The present study investigated whether fractionated radiation influences the metabolism of GSCs.

Methods

Cell culture

Cells were isolated from tumors formed by implantation of *Ink4/Arf*-null neural stem/progenitor cells transduced with $HRAS^{V12}$ into the forebrain of wild-type mice. The cells were sorted for green fluoresence protein (GFP) fluorescence (tumor spheres: TS), and TS were subjected to a regimen of 12 fractions of 5 Gy of ionizing radiation (TS-RR). This method is described in detail elsewhere.[7] Clones obtained from TS and TS-RR by single-cell cloning, also previously described,[7] were numbered sequentially and five representative clones from each group (low radioresistance TS clones: numbers 2, 4, 6, 7, 12; high radioresistance TS-RR clones: numbers 10, 17, 22, 25, 26) were used in the subsequent analysis in this study.

All cells were cultured in neural stem cell medium (NSM) consisting of Dulbecco's Modified Eagle's medium/F-12 (Sigma-Aldrich Corp., St. Louis, MO, USA) supplemented with recombinant human epidermal growth factor (20 ng/ml) (PeproTech Inc., Rocky Hill, NJ, USA), recombinant human basic fibroblast growth factor (20 ng/ml) (PeproTech), B27 supplement without vitamin A (Invitrogen, Carlsbad, CA, USA), heparan sulfate (200 ng/ml), penicillin (100 U/ml), and streptomycin (100 ng/ml) (Nacalai Tesque Inc., Kyoto, Japan).

Orthotopic implantation

Orthotopic implantation of tumor cells was performed as previously described.[8] All animal experiments were approved by the Institutional Animal Care and Use Committee of Keio University School of Medicine (Study no. 11020).

In vitro irradiation

TS and TS-RR clones were exposed to 5 Gy of ionizing radiation with the use of an X-irradiator (Hitachi MBR-1520R-3; Hitachi Medical Corp., Tokyo, Japan) with settings of 150 kV and 20 mA.

Colony formation assay

Clonogenic survival after irradiation was evaluated by colony formation assay, as previously described.[7] In brief, cells were embedded in 0.5% agarose and allowed to settle for 24 h before irradiation. Two weeks after irradiation with 5 Gy, the cells were fixed with 4% paraformaldehyde and stained with toluidine blue O (Sigma-Aldrich). The wells were photographed, and the spheres were counted manually.

Tissue histology

Tissue was fixed overnight with 4% paraformaldehyde, embedded in paraffin, and sectioned at a thickness of 4 μm. Sections were depleted of paraffin and stained with hematoxylin and eosin.

Reverse transcription and real-time polymerase chain reaction analysis

Total ribonucleic acid (RNA) was isolated from cells with the use of an RNeasy Mini Kit (Qiagen N.V., Venlo, Netherlands), and portions of the RNA (1 μg) were subjected to reverse transcription (RT) with a PrimeScript™ RT reagent kit (Takara Bio Inc., Kusatsu, Shiga, Japan). The resulting complementary deoxyribonucleic acid (cDNA) was subjected to real-time polymerase chain reaction (PCR) analysis with the use of SYBR® *Premix Ex Taq*™ II (Takara Bio) and a Thermal Cycler Dice® Real Time System (TP800, Takara Bio). Mouse primer sequences (forward and reverse, respectively) were as follows: *Actb*, 5'-CCACTGCCGCATCCTCTTCC-3' and 5'-GCCACAGGATTCCATACCCAAGA-3'; *Igf1r*, 5'-TTGTGTTGTTCGTCCGGTGTG-3' and 5'-ATGTGCCCAAGTGTGTGCG-3'. Data for *Igf1r* messenger RNA (mRNA) were normalized by the corresponding amount of *Actb* mRNA.

Immunoblot analysis

Total protein was extracted from cells by repeated passage through a 25-gauge needle in radioimmunoprecipitation (RIPA) buffer (Sigma-Aldrich). Target proteins were detected with antibodies to IGF1Rβ, to the phosphorylated or total forms of AKT (Cell Signaling Technology Inc., Danvers, MA, USA), or to β-actin (Santa Cruz Biotechnology Inc., Dallas, TX, USA) and then with horseradish peroxidase-conjugated secondary antibodies followed by enhanced chemiluminescence reagents (Nacalai Tesque).

Lactate production, glucose consumption, and adenosine triphosphate content

Cellular lactate production was measured with the use of a Lactate Assay Kit II (BioVision Inc., Milpitas, CA, USA), glucose consumption was measured with a Glucose Assay Kit GAGO-20 (Sigma-Aldrich), and intracellular adenosine triphosphate (ATP) level was measured with a CellTiter-Glo® Luminescent Cell Viability Assay (Promega Corp., Madison, WI, USA). Absorbance or luminescence was recorded with the use of a microplate reader (Synergy 4; BioTek Instruments Inc., Winooski, VT, USA) and was normalized by cell number.

Extracellular flux analysis

The extracellular acidification rate (ECAR) and oxygen consumption rate (OCR) were determined with the use of a Seahorse XF^e Extracellular Flux Analyzer (Seahorse Bioscience, North Billerica, MA, USA). In brief, 24-well plates were coated with BD Matrigel™ (BD Biosciences, San Jose, CA, USA) diluted 1:10 in extracellular flux (XF) Assay Medium (Seahorse Bioscience). Dissociated cells were plated at a density of 80000 per well in NSM, allowed to attach to the plate, and then incubated in XF Assay Medium supplemented with 17.5 mM glucose and 1 mM pyruvate for 1 h before the assay.

Metabolome analysis

For extraction of metabolites, cells were collected, centrifuged at 1200 rpm for 5 min, and washed with 10 ml of 5% mannitol. After the addition of 1 ml of methanol containing D,L-methionine sulfone (Tokyo Chemical Industry Co., Ltd. (TCI), Tokyo, Japan), 2-morpholinoethanesulfonate (Dojindo Laboratories, Kamimashiki, Kumamoto, Japan), and the sodium salt of D-camphor-10-sulfonic acid (Wako Pure Chemical Industries Ltd., Osaka, Japan), each at 25 μM as internal standards, 400 μl of homogenate was mixed with 400 μl of chloroform and 200 μl of deionized water. The mixture was centrifuged at 10000 × *g* for 3 min at 4℃, after which 400 μl of the aqueous layer was purified and concentrated by ultrafiltration and centrifugation at 9100 × *g* for 3 h at 4℃. The filtrate was immediately stored at −80℃ until analysis by capillary electrophoresis and time-of-flight mass spectrometry (CE-TOFMS), as previously described.[9–11] Samples were prepared in quadruplicate, and metabolite levels were normalized by cell number, as determined from a parallel sample.

Statistical analysis

Data are presented as bar charts with error bars indicating standard deviation and were analyzed with the unpaired Student *t* test as performed with Excel (Microsoft Corp., Redmond, WA, USA). Kaplan-Meier survival analysis was performed with the use of the JMP7 software package (SAS Institute Inc., Cary, NC, USA). A p value of <0.05 was considered statistically significant.

Results

To investigate the effect of fractionated radiation on GSC metabolism, we adopted our previously described murine malignant glioma model and selected five clonal populations representing GSCs — TS clone numbers 2, 4, 6, 7, and 12 — and five clonal populations representing GSCs subjected to fractionated radiation — TS-RR clone numbers 10, 17, 22, 25, and 26[7] — for metabolic analysis.

To confirm that the clonal populations retained the features of the parental populations, TS and TS-RR, we first examined the colony-forming ability of clones after they were exposed to a single 5-Gy dose of ionizing radiation. Consistent with the characteristics of the parental cells,[7] TS-RR clones formed more colonies than did their TS counterparts (Fig. 1A). TS-RR clones also exhibited a slower rate of proliferation, as determined by the survival of mice subjected to intracranial implantation of the cell clones (Fig. 1B). Moreover, the tumors formed by TS-RR clones retained all pathognomonic features of the TS-derived tumors (Fig. 1C).

The two types of clones also mirrored the patterns of IGF1R expression and AKT phosphorylation observed in the bulk populations: TS-RR clones manifested greater amounts of *Igf1r* mRNA and IGF1R protein and most TS clones had higher levels of AKT phosphorylation (Fig. 2).

We next examined whether the metabolic characteristics of TS-RR clones differed from those of TS clones. Glucose consumption (Fig. 3A) and lactate production (Fig. 3B) were significantly lower in TS-RR clones than in TS clones, and intracellular ATP content was also slightly lower in TS-RR clones (Fig. 4A). Examination of extracellu-

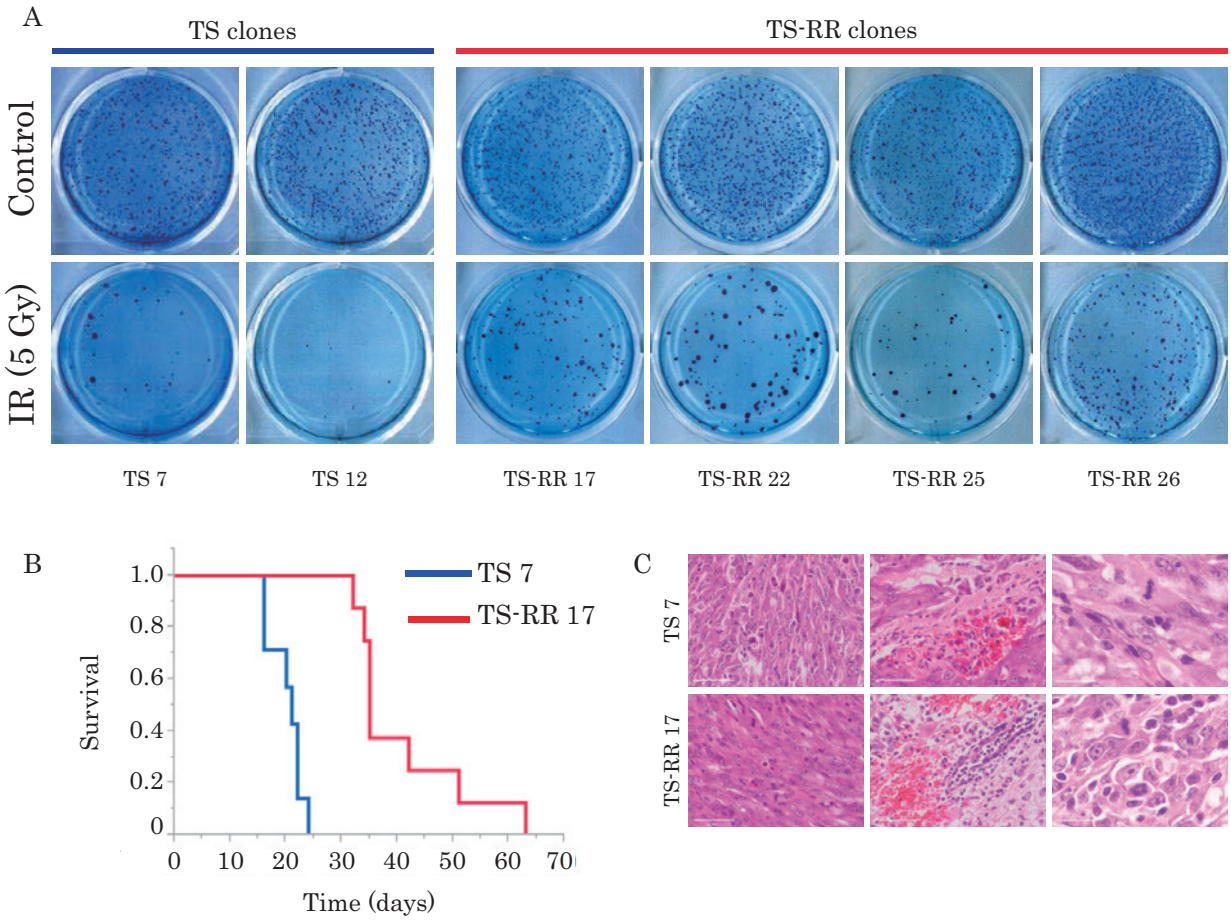

Fig. 1 Colony formation *in vitro* and tumor formation *in vivo* by tumor spheres (TS) and TS-RR clones.
A: Clonogenic survival assay for TS and TS-RR clones subjected (or not, control) to irradiation (IR) with a single dose of 5 Gy. Representative images of colonies formed 2 weeks after irradiation are shown.
B: Survival curves for wild-type mice subjected to orthotopic implantation of 1000 cells of TS clone number 7 (n = 7) or TS-RR clone number 17 (n = 8).
C: Hematoxylin-eosin staining of tumors formed by TS clone number 7 or TS-RR clone number 17 at 22 days after intracranial implantation. The panels show high cellularity and atypia (left), hemorrhage and invasion of surrounding brain tissue (middle), and mitosis and cellular heterogeneity (right). Scale bars: 50 μm (left and middle) or 20 μm (right).

lar metabolite flux in a single pair of clones revealed that the extracellular acidification rate (ECAR) and oxygen consumption rate (OCR) were significantly lower in TS-RR clone number 17 than in TS clone number 7 (Fig. 4B).

Our results showed that GSCs subjected to fractionated radiation possessed metabolic characteristics distinct from those of the nontreated stem cell population and a lower rate of aerobic glycolysis. To examine the intracellular metabolic characteristics in more detail, we performed a metabolome analysis of all 10 TS and TS-RR clones. Consistent with the results for extracellular metabolites, intracellular concentrations of glycolytic intermediates such as glucose 6-phosphate, fructose 1,6-bisphosphate, and lactate were significantly lower in the TS-RR clone group (Fig. 5 A). Furthermore, TS-RR clones manifested lower levels of intermediates of the pentose phosphate pathway, such as ribulose 5-phosphate and sedoheptulose 7-phosphate (Fig. 5B). Although nucleoside levels were not evaluable in all quadruplicate samples of all clones, concentrations of nucleoside monophosphates were significantly lower in TS-RR clones than in TS clones (Fig. 6A). In contrast, no specific metabolite groups showed an increased abundance in the radioresistant clones. However, levels of essential amino acids such as isoleucine, methionine, and tryptophan did not differ significantly between TS and TS-RR clones (Fig. 6B).

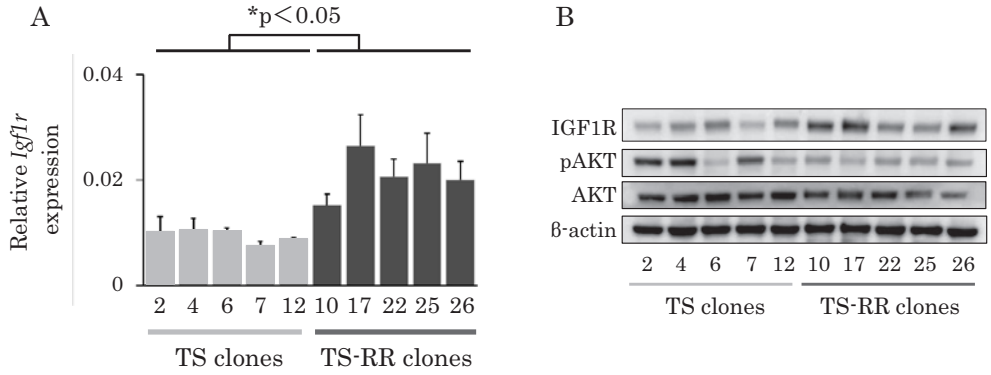

Fig. 2 Insulin-like growth factor 1 receptor (IGF1R) expression and AKT phosphorylation in tumor spheres (TS) and TS-RR clones.
A: Reverse transcription (RT) and real-time polymerase chain reaction (PCR) analysis of *Igf1r* messenger ribonucleic acid (mRNA) in TS and TS-RR clones. Data are means of triplicates from a representative experiment.
B: Immunoblot analysis of IGF1R, Ser^{473}-phosphorylated AKT (pAKT), total AKT, and β-actin (loading control) in TS and TS-RR clones.

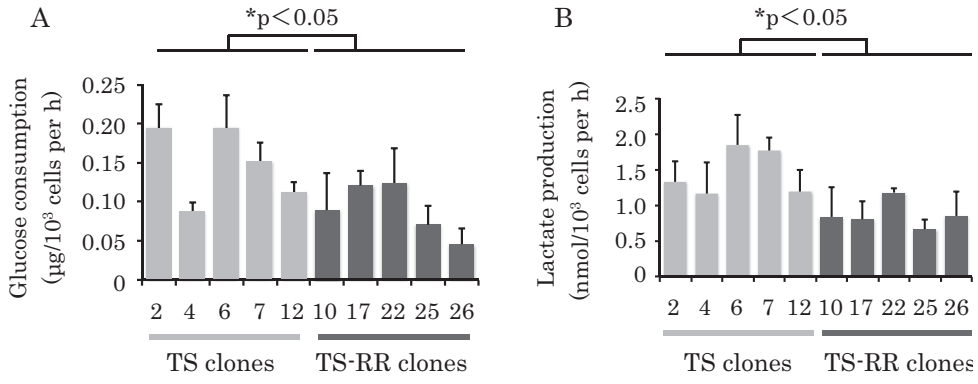

Fig. 3 Glucose consumption **(A)** and lactate production **(B)** by tumor spheres (TS) and TS-RR clones. Data are the means of two independent experiments.

Discussion

We previously showed that fractionated radiation induced multiple phenotypic changes in GSCs, including a decrease in proliferation rate and an increase in resistance to subsequent irradiation.[7] In the present study, we investigated whether this change in proliferation rate was accompanied by changes in bioenergetic status and the metabolic parameters used to detect recurrent lesions. We found that glycolytic flux was markedly lower in GSCs exposed to fractionated radiation than in nontreated GSCs. Furthermore, although the abundance of no specific metabolite group was higher in irradiated cells than in nontreated GSCs, levels of essential amino acids, including isoleucine, methionine, and tryptophan, did not significantly differ between the two types of clones.

Our findings highlight a less-described aspect of GSC biology, namely, GSC metabolic characteristics before and after fractionated radiation. The cells that eventually initiate disease recurrence — cancer stem cells — have the greatest tumorigenic ability but are thought to be more quiescent than bulk tumor cells. In our murine glioblastoma model, fractionated radiation further slowed GSC proliferation, which suggests that their metabolism may also be slowed. Indeed, the quiescent and proliferating states of lymphocytes, for example, differ markedly in their reliance on glycolysis.[12] However, quiescence induced by contact inhibition is not accompanied by a sub-

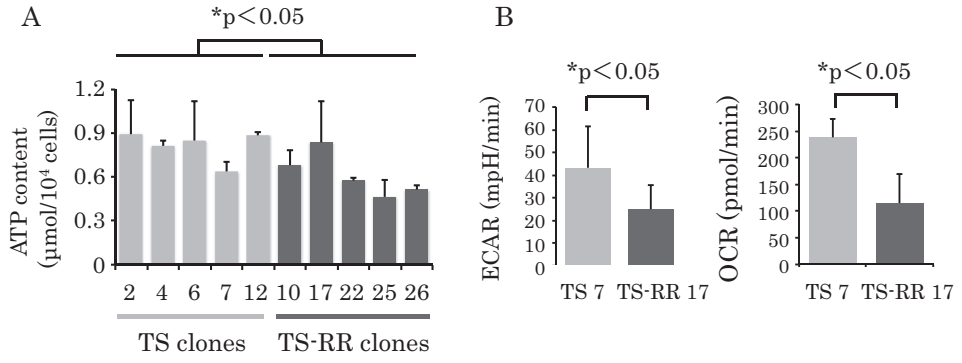

Fig. 4 Adenosine triphosphate (ATP) content in tumor spheres (TS) and TS-RR clones **(A)** and extracellular acidification rate (ECAR) and oxygen consumption rate (OCR) for TS clone number 7 and TS-RR clone number 17 **(B)**. For **(A)**, data are the means of two independent experiments.

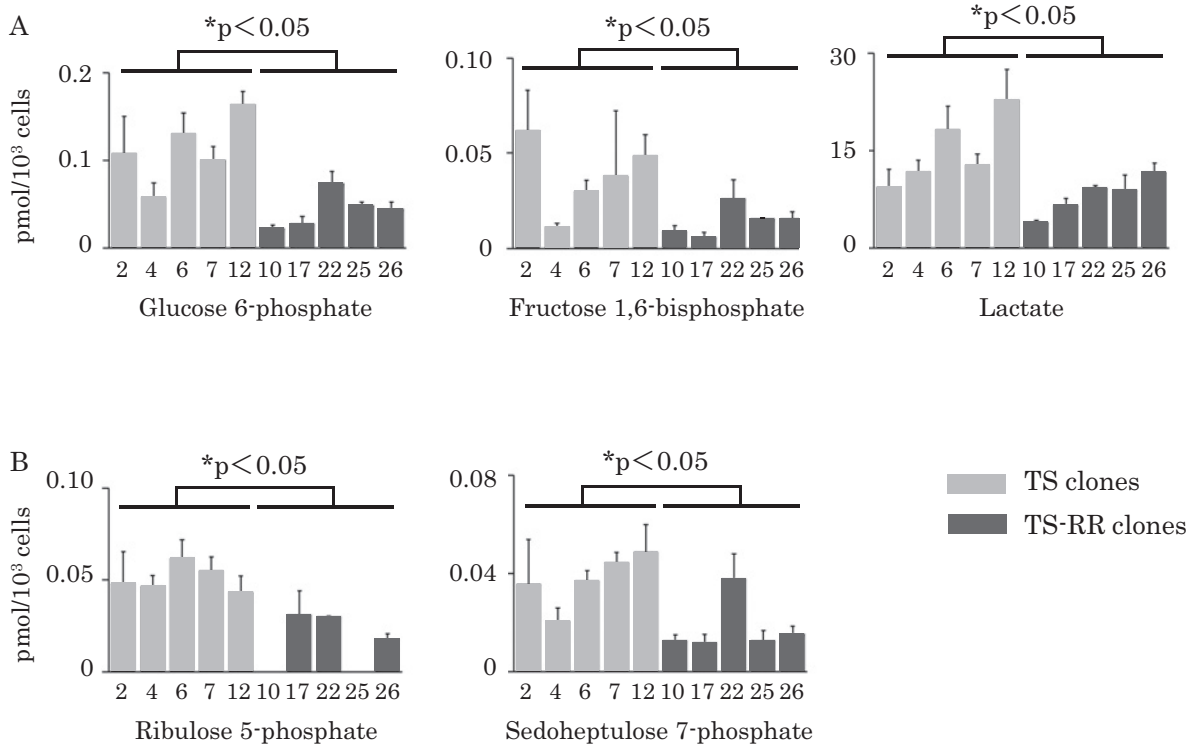

Fig. 5 Metabolome analysis of intracellular levels of intermediates of glycolysis **(A)** and the pentose phosphate pathway **(B)** in tumor spheres (TS) and TS-RR clones. Data are the means of quadruplicate samples.

stantial slowing of metabolism and glucose uptake in fibroblasts.[13] Furthermore, cells that survive treatment or oncogene ablation have been shown to manifest stem cell–like properties and to rely on oxidative phosphorylation.[14, 15] We found that GSCs subjected to fractionated radiation exhibited a decrease in glucose and oxygen consumption, without an equivalent decrease in ATP content. These findings may reflect a decrease in ATP production and consumption or a switch in the main carbon source and energy pathway. Our model system seems to support

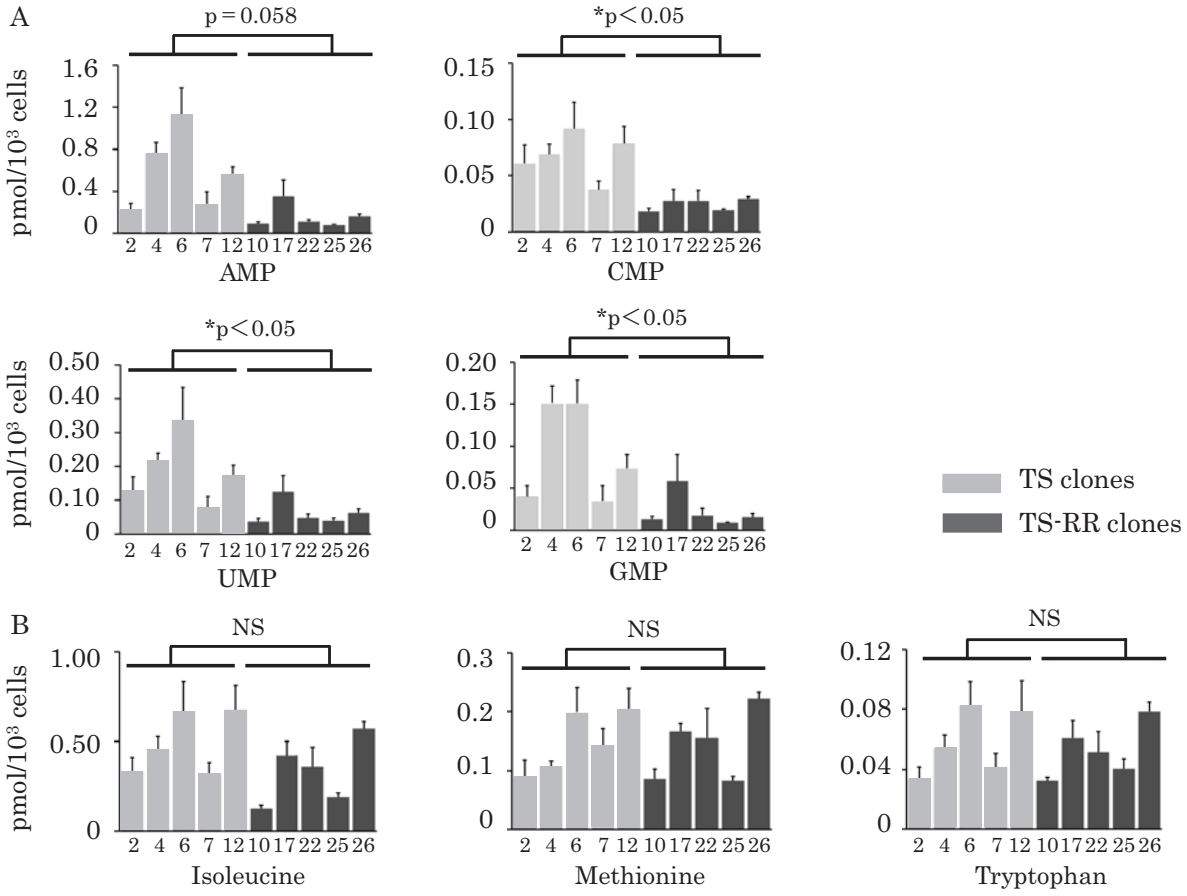

Fig. 6 Metabolome analysis of intracellular levels of nucleoside monophosphates **(A)** and the indicated essential amino acids **(B)** in tumor spheres (TS) and TS-RR clones. Data are the means of quadruplicate samples.
NS: not significant
AMP: adenosine 5'-monophosphate, CMP: cytidine 5'-monophosphate, UMP: uridine 5'-monophosphate, GMP: guanosine 5'-monophosphate

the former hypothesis, given the reduced proliferation rate, the observed decrease in the abundance of intermediates of nucleoside metabolism, and the apparent absence of an increase in any particular carbon-source metabolite or pathway in the TS-RR clones.

From a diagnostic point of view, a major challenge in identifying recurrent cancer lesions is detection of the presence of a small number of tumor stem cells within an environment that has also undergone several treatment-induced changes. In the present study, we also examined whether any of the metabolites used in imaging for recurrent lesions was influenced by the reduced proliferation rate of TS-RR cells. Amino acid－based PET has shown promise in malignant glioma imaging,[1, 16] as the uptake of tracers based on methionine, tyrosine, or tryptophan has been quantified to identify metabolically active glioma cells. The intracellular levels of amino acids (including essential amino acids) determined in our study represent the net balance between uptake and consumption; however, they did not differ significantly between TS and TS-RR clones and might therefore be of use in identifying even radioresistant GSCs. Further analysis of GSCs isolated from mice after irradiation *in vivo* or those derived from clinical samples might help identify metabolites specifically enriched in GSCs that survive therapy.

Our findings that post-radiation GSCs exhibit a decrease in glucose consumption and maintain relatively similar levels of intracellular amino acids have therapeutic implications. In recent years, metabolic targeting is considered a valuable new treatment strategy. While multiple options

exist, preclinical studies have targeted glycolysis, nucleic acid synthesis, and amino acid synthesis,[17] and the results depended on tumor type and the timing of the intervention. Because irradiated GSCs show a decline in glycolysis, our results suggest that the use of glycolysis inhibitors might be less effective when used after radiation therapy for malignant glioma. In contrast, the relative maintenance of intracellular essential amino acid levels suggests a continued need for these specific compounds in GSCs. Future experiments should attempt to determine possible amino acid dependencies for irradiated GSCs and to exploit the identified key amino acids in diagnosis PET and treatment.

Our results suggest that repeated radiation changes the metabolic preferences of GSCs in conjunction with their slowed proliferation. Further investigations of intra- and extracellular metabolites should attempt to identify potential targets for detection and treatment of recurrent lesions.

We express our gratitude to Professors Hideyuki Saya (Division of Gene Regulation, IAMR, Keio University School of Medicine) and Satoshi Iwabuchi (Department of Neurosurgery (Ohashi), School of Medicine, Faculty of Medicine, Toho University) for their guidance and supervision of the research and manuscript preparation. We thank I. Ishimatsu for preparing samples for histopathology and the Collaborative Research Resources, School of Medicine, Keio University, for technical assistance.

Conflicts of interest: No conflict of interest to declare.

References

1) Dhermain FG, Hau P, Lanfemann H, Jacobs AH, van den Bent MJ. Advanced MRI and PET imaging for assessment of treatment response in patients with gliomas. Lancet Neurol. 2010; 9: 906-20.
2) Warburg O. On the origin of cancer cells. Science. 1956; 123: 309-14.
3) Vander Heiden MG, Cantley LC, Thompson CB. Understanding the Warburg effect: the metabolic requirements of cell proliferation. Science. 2009; 324: 1029-33.
4) Mao P, Joshi K, Li J, Kim SH, Li P, Santana-Santos L, et al. Mesenchymal glioma stem cells are maintained by activated glycolytic metabolism involving aldehyde dehydrogenase 1A3. Proc Natl Acad Sci USA. 2013; 110: 8644-9.
5) Vlashi E, Lagadec C, Vergnes L, Matsutani T, Masui K, Poulou M, et al. Metabolic state of glioma stem cells and nontumorigenic cells. Proc Natl Acad Sci USA. 2011; 108: 16062-7.
6) Saga I, Shibao S, Okubo J, Osuka S, Kobayashi Y, Yamada S, et al. Integrated analysis identifies different metabolic signatures for tumor-initiating cells in a murine glioblastoma model. Neuro Oncol. 2014; 16: 1048-56.
7) Osuka S, Sampetrean O, Shimizu T, Saga I, Onishi N, Sugihara E, et al. IGF1 receptor signaling regulates adaptive radioprotection in glioma stem cells. Stem Cells. 2013; 31: 627-40.
8) Sampetrean O, Saga I, Nakanishi M, Sugihara E, Fukaya R, Onishi N, et al. Invasion precedes tumor mass formation in a malignant brain tumor model of genetically modified neural stem cells. Neoplasia. 2011; 13: 784-91.
9) Soga T, Ohashi Y, Ueno Y, Naraoka H, Tomita M, Nishioka T. Quantitative metabolome analysis using capillary electrophoresis mass spectrometry. J Proteome Res. 2003; 2: 488-94.
10) Soga T, Igarashi K, Ito C, Mizobuchi K, Zimmerman HP, Tomita M. Metabolomic profiling of anionic metabolites by capillary electrophoresis mass spectrometry. Anal Chem. 2009; 81: 6165-74.
11) Hirayama A, Kami K, Sugimoto M, Sugawara M, Toki N, Onozuka H, et al. Quantitative metabolome profiling of colon and stomach cancer microenvironment by capillary electrophoresis time-of-flight mass spectrometry. Cancer Res. 2009; 69: 4918-25.
12) Valcourt JR, Lemons JMS, Haley EM, Kojima M, Demuren OO, Coller HA. Staying alive: metabolic adaptations to quiescence. Cell Cycle. 2012; 11: 1680-96.
13) Lemons JMS, Feng XJ, Bennett BD, Legesse-Miller A, Johnson EL, Raitman I, et al. Quiescent fibroblasts exhibit high metabolic activity. PLoS Biol. 2010; 8: e1000514.
14) Haq R, Shoag J, Andreu-Perez P, Yokoyama S, Edelman H, Rowe GC, et al. Oncogenic BRAF regulates oxidative metabolism via PGC1α and MITF. Cancer Cell. 2013; 23: 302-15.
15) Viale A, Pettazzoni P, Lyssiotis CA, Ying H, Sánchez N, Marchesini M, et al. Oncogene ablation-resistant pancreatic cancer cells depend on mitochondrial function. Nature. 2014; 514: 628-32.
16) Bosnyák E, Kamson DO, Robinette NL, Barger GR, Mittal S, Juhász C. Tryptophan PET predicts spatial and temporal patterns of post-treatment glioblastoma progression detected by contrast-enhanced MRI. J Neurooncol. 2016; 126: 317-25.
17) Vander Heiden MG. Targeting cancer metabolism: a therapeutic window opens. Nat Rev Drug Discov. 2011; 10: 671-84.